

Benard Surface-Tension-Driven Convection in Small Vessels

M.J. Medale¹, P.J. Cerisier¹

1

Summary

This study is focused on the confinement influence on the characteristics of the Bénard surface-tension-driven convection: threshold, bifurcations, stable or dynamical regimes and patterns. A numerical model has been developed to deal with containers of any shapes and sizes, which represents a significant step in the numerical study of this class of problems. It is based on a finite element method and second-order approximation of the primary variable fields. Steady state and transient solution algorithms have been implemented together with a continuation solution algorithm to follow branches of solutions and locate eventual bifurcation. We present results of just-critical and slightly supercritical regimes (up to $1.6 Ma_c$) for silicon oil layers ($Pr = 880$ at $25\text{ }^\circ\text{C}$) in containers of small to moderate aspect ratio ($2 < \Gamma < 25$) and of various shape (triangular, square, pentagonal, hexagonal and circular).

Introduction

One of the main objectives in studying surface-tension-driven convection in containers is to understand the influence of the confinement on the convective pattern characteristics (threshold, stable regimes, etc.). Does the hexagonal pattern, which exists in very large aspect ratios (defined as the horizontals extend to the depth of the liquid layer), still exist in confined configurations? Could a particular container shape allow the hexagonal pattern to exist in small vessels? As each lateral wall of a polygonal container attempts to impose its own orientation to the adjacent hexagonal pattern (the adjacent cell boundary lying along the lateral wall must be perpendicular to it), some vessels (regular hexagons and triangles) are expected to be compatible with respect to the hexagonal pattern. Conversely, vessels of other shape such (squares, pentagons) don't meet this requirement. Experimental evidence has been shown in [1,2].

Surface-tension-driven convection in confined containers has only been numerically studied in square (or rectangular) and circular vessels. This is mainly due to the inadequacy of the currently used numerical techniques to deal with other container shapes. The numerical model we have developed aims to overcome this geometrical limitation since it enables us to get a solution in containers of any shape. Furthermore, it features the computation of the threshold value and its associated pattern, steady supercritical solutions, subsequent

¹ University of Provence, Marseilles, France.

bifurcations together with unsteady or transient regimes. In the present study, we have numerically investigated the dependence of the convective cellular pattern on the shape of the container, for small to moderate aspect ratios.

Governing Equations

We consider the incompressible flow of a Newtonian fluid bounded at its lower part by a solid wall, considered isothermal (at $T=T_h$), and at its upper part by a thin layer of air, which is at its turn topped by another isothermal solid wall (at $T=T_c < T_h$). The liquid layer is assumed horizontal and the liquid-air interface is presumed flat. The problem is governed by the coupled incompressible Navier-Stokes equations and energy equation, in the Boussinesq approximation [7].

Numerical Model

The developed code has been designed to provide interesting capabilities of physical relevance, while achieving satisfactory computational accuracy and efficiency to get three-dimensional transient and/or steady state solutions (which were not considered in [7]). In order to get the desired flexibility in spatial discretisation we have favoured the finite element method to develop our numerical model. Furthermore, when looking for the computational efficiency it is of first concern to give prominence to the compatibility between the problem formulation, the selected solution algorithms or strategies and finally the computer architecture and programming environment. For that reason we have implemented two separate formulations (and their associated solution algorithms) in our code. The first one is specially devoted to the steady state solutions, while the second one is designed to deal efficiently with transient solutions. The developed code has been designed to run high performance computers, taking advantage of parallel processing. It has been written on top of the Petsc library [3] in order to reach the hard trade off between performance and ease to develop.

When a steady state solution actually exists, it can be computed thanks to a fully coupled formulation. On the other hand, we are also interested either in some transient solutions (cells organization) or solutions for which no steady state exists at all (dynamical regimes). The implemented transient solution algorithm consists in separate finite element formulations for the heat transfer and the fluid-flow problems. The incompressible fluid flow component is undertaken with an unconditionally stable projection algorithm [4], which consists in splitting the incompressible fluid flow problem into two algebraic systems, one for the momentum equation and another one for the pressure correction associated with the incompressibility constraint.

In order to start the computations we have chosen initial fields that shouldn't *a priori* influence the solutions. For all steady state computations the linearised algebraic system is solved at each iteration of the Newton-Raphson procedure with an efficient parallel direct solver [5]. A continuation procedure (based on an Asymptotic Numerical Method [6] is used to follow branches of steady state. For the transient computations, the implemented segregated solution algorithm consists in solving the three algebraic systems in a consecutive manner, at each time step. The algebraic system associated with the momentum is linearized with a Newton-Raphson method, accelerated with a cubic line search technique.

The numerical model has been validated with respect to several reference computations and experiments, and a very good agreement was obtained [7].

Results

We have analyzed several configurations for different container shapes (hexagonal, pentagonal, triangular), and various aspect ratio containers $2 < \Gamma < 25$ ($\Gamma = \sqrt{S} / d$, S: free surface area, d: liquid layer depth). We consider a silicon oil layer ($Pr = 880$ at $25^\circ C$, $d=1$ mm), so buoyancy is negligible with respect to surface-tension forces ($Ra = 0$). The Biot number which characterizes the heat transfer across the liquid-air interface is taken equal to $Bi = 0.1$.

Figure 1 shows the plot of $\delta\epsilon$ versus Γ , where $\delta\epsilon = (Mac - Mac_\infty) / Mac_\infty$ and Mac is the critical Marangoni number for the considered container and Mac_∞ its value for an infinite layer ($Mac_\infty = 83.1$ for $Bi = 0.1$). It is noteworthy to observe two main zones on this plot: i) for $\Gamma < 3.5$ the slope is very steep. This case corresponds to the case where only one cell fills the whole container. The shape of the container plays also an important part: for a given Γ , Mac increases as the number of the polygonal walls decreases; ii) for $\Gamma > 3.5$ the curves tend asymptotically towards 0 (infinite layer limit); so the plot is restricted to $\Gamma = 10$.

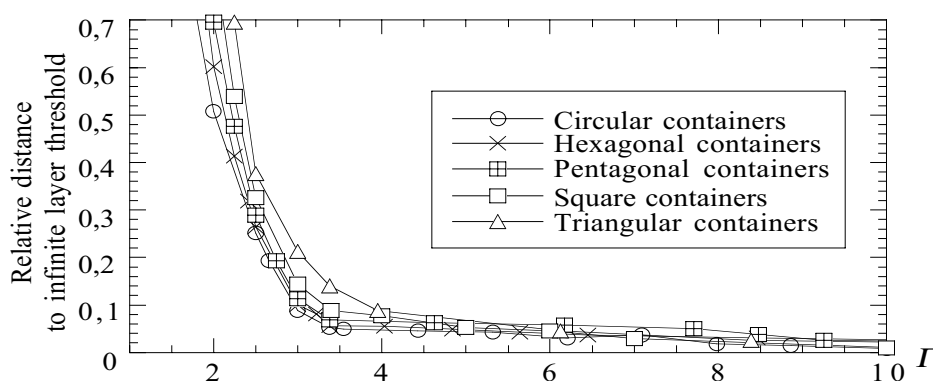


Figure 1: Threshold values versus aspect ratio for various container shapes.

Figures 2-4 present the evolution of steady state convective patterns as Γ increases for the considered containers. Four main regions can be distinguished: i) for $\Gamma < 3.5$ a single cell appears in the container, it possesses its geometry (shape and size); the velocity and temperature fields at the free surface display an axial symmetry in the central part of the hexagonal and pentagonal containers, whereas they present a ternary symmetry in the triangular one. ii) for $3.5 < \Gamma \leq 7.5$, from two up six convective cells in contact to lateral wall exist. The cells in the peripheral row are strongly influenced by the container shape. iii) for $\Gamma \approx 7.5$, the central cell is most likely to be a hexagonal or a pentagonal one. iiiii) for $\Gamma > 7.5$ the pattern consists in a central core of hexagonal cells surrounded with a row of predominantly pentagonal ones.

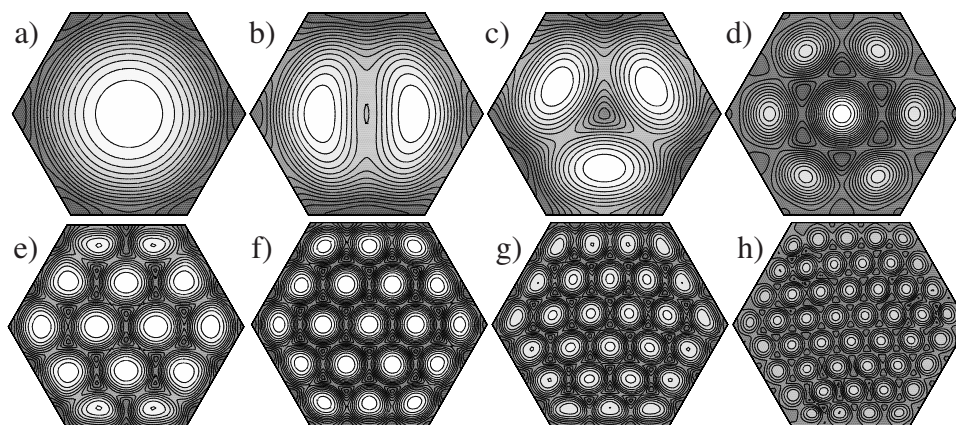


Figure 2. Free surface temperature field for various hexagons: a) $\Gamma=3.0$; b) $\Gamma=5.0$; c) $\Gamma=6.0$; d) $\Gamma=10.4$; e) $\Gamma=14.0$; f) $\Gamma=17.5$; g) $\Gamma=21.0$; h) $\Gamma=27.75$.

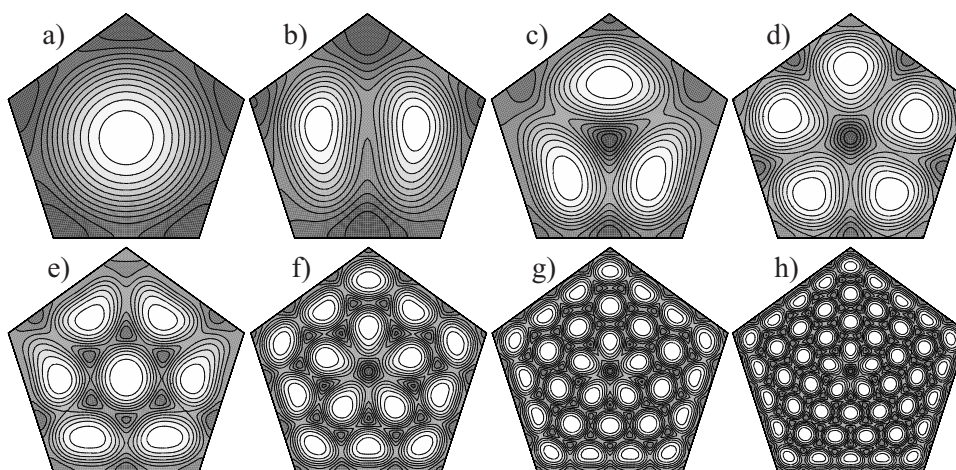


Figure 3. Free surface temperature field for various pentagons: a) $\Gamma=3.0$; b) $\Gamma=4.6$; c) $\Gamma=6.2$; d) $\Gamma=7.7$; e) $\Gamma=9.25$; f) $\Gamma=13.4$; g) $\Gamma=18.5$; h) $\Gamma=23.6$.

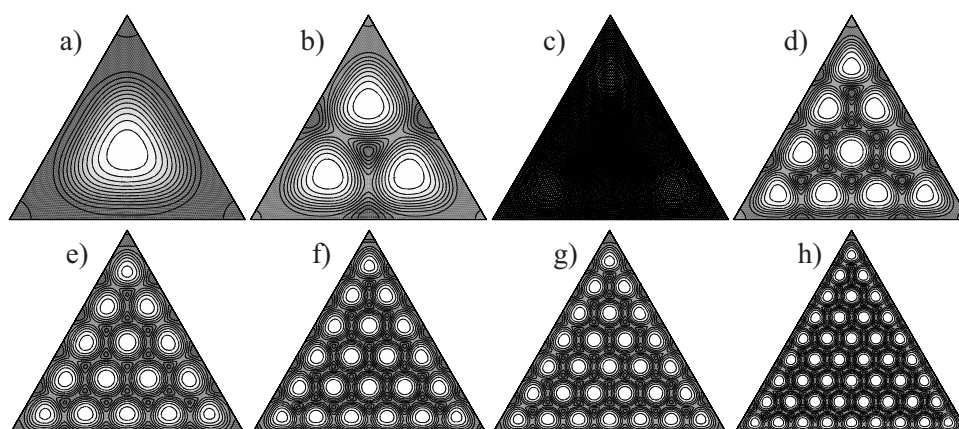


Figure 4. Free surface temperature field for various triangles: a) $\Gamma=3.0$; b) $\Gamma=6.1$; c) $\Gamma=8.4$; d) $\Gamma=10.7$; e) $\Gamma=12.9$; f) $\Gamma=15.2$; g) $\Gamma=17.5$; h) $\Gamma=22.0$.

It could be underlined that even in moderate aspect ratio, a perfect hexagonal pattern can be attained in compatible vessels (see figure 5 for hexagonal and triangular containers) provided a size compatibility condition is fulfilled (the container perimeter matches an integer times the cell size).

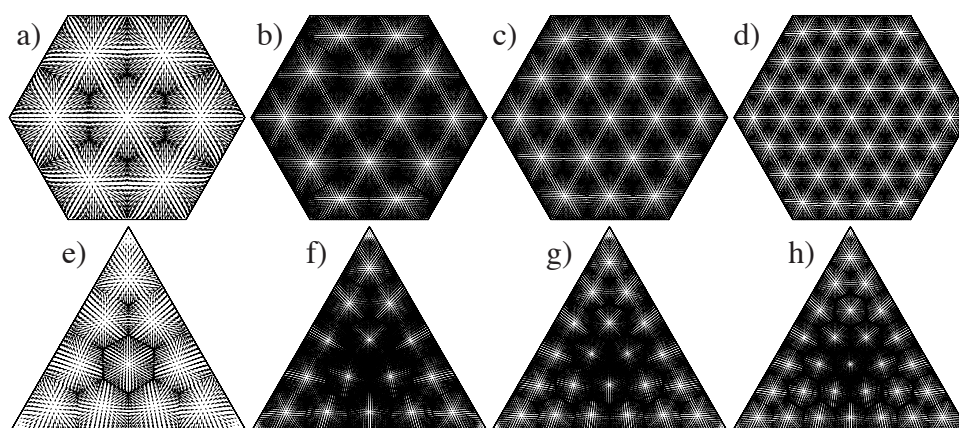


Figure 5. Free surface velocity field for several hexagonal and triangular containers: a) $\Gamma=10.4$; b) $\Gamma=14$; c) $\Gamma=17.5$; d) $\Gamma=24.5$; e) $\Gamma=10.7$; f) $\Gamma=12.9$; g) $\Gamma=15.2$; h) $\Gamma=17.5$.

Conclusion

We have developed a powerful and accurate numerical model to investigate the Bénard convection in small to medium aspect ratio containers of various shapes. The present study outlines how the container geometry can affect the cellular flow pattern and its associated characteristics (threshold, secondary

bifurcations and patterns). An hysteresis behavior of the Marangoni number has been observed in all cases around the threshold, confirming the intrinsic characteristic of Bénard surface-tension-driven flows. The obtained steady state patterns evolve progressively for increasing aspect ratio, from only one cell (inheriting the container shape), several wall-cells, a single central-core-cell (intrinsic cell) surrounded with wall-cells, and finally a central zone made up of intrinsic-cells surrounded with wall-cells. On the other hand dynamical regimes have been shown to exist even close to the threshold, provided a combination of geometrical and physical parameters fulfills a suggested criterium.

The first author thanks CNRS for providing substantial computing resources on the its Cray T3E and IBM SP4 supercomputers at IDRIS, Orsay (France).

Reference

1. Cerisier, P., Pérez-Garcia, C., Jamond, C. and Pantaloni, J. (1987): "Wavelength Selection In Bénard-Marangoni Convection", *Phys. Rev. A* 35, pp. 1949-1952.
2. Koschmieder, E. L. and Prahl, S. A. (1990): "Surface Tension Driven Bénard Convection In Small Containers", *J. Fluid Mech.*, Vol. 215, pp 571-583.
3. Balay, S., Gropp, W., McInnes, L. C., and Smith, B. (1998): "Petsc 2.0.21 Users Manual" ([Http://Www-Fp.Mcs.Anl.Gov/Petsc/](http://www-fp.mcs.anl.gov/petsc/)), Mathematics And Computer Science Division, Argonne National Laboratory.
4. Guermond, J. L. and Quartapelle, L. (1997): "Calculation of Incompressible Viscous Flows by an Unconditionally Stable Projection Fem", *J. Comp. Physics*, Vol. 132, pp. 12-33.
5. Aschcraft, C. and Grimes, R. (1999): "Spooles: An Object-Oriented Sparse Matrix Library". In *Siam Conference On Parallel Processing For Scientific Computing*.
6. Baguet, S. and Cochelin, B. (2003): "On the behaviour of the ANM continuation in the presence of bifurcations", *Commun. Numer. Meth. Engng*, Vol. 19, pp. 459-471.
7. Medale, M. and Cerisier, P. (2002): "Numerical Simulation of Bénard-Marangoni convection in small aspect ratio containers". *Num. Heat. Trans. A* Vol. 42, pp. 55-72.